A model for electrode effects based on adsorption theory

A model for electrode effects based on adsorption theory

A. S. Gliozzi[a], S. Hernández[a,c], A. L. Alexe-Ionescu[a,b], G. Saracco[a], G. Barbero[a]

[a] *Department of Applied Science and Technology (DISAT), Politecnico di Torino, Corso Duca degli Abruzzi 29, 10129 Torino, Italy.*
[b] *Department of Physics, University Politehnica of Bucharest, Splaiul Independentei 313, 060042 Bucharest, Romania.*
[c] *Center for Space Human Robotics (IIT@POLITO),Istituto Italiano di Tecnologia, Corso Trento 21, 10129, Torino, Italy.*

Abstract

A model to describe the electrode effects based on the adsorption theory is proposed. We assume that the coverage (i.e by gas bubbles, electrodeposition of compounds, etc) of the electrodes is governed by a kinetics equation where the adsorption term is proportional to the bulk current density, and the desorption term to the actual coverage. The adsorption can take place only on the uncovered part of the electrode. We show that the coverage is responsible for a variation of the interface properties of the electrode. The time dependence of the electric response of the cell, submitted to an external voltage, is determined by solving the differential equation for the coverage. We show that two regimes are expected. One, in the limit of small time, controlled by the charging of the surface interface, and one related to the coverage. The theoretical predictions are in reasonable agreement with the experimental data concerning the time dependence of the current and the current-voltage characteristics of a home-made photo-electrolyzer constituted by a $BiVO_4$ photoanode and a Pt cathode. Moreover, a normalized current-voltage curve was obtained, which fit also literature data based on (i) electrolysis on cylindrical stainless-steel electrodes in $NaOH$ electrolyte and (ii) electrolytic plasma nitrocarburizing of AISI 1020 steel discs in an Urea-based aqueous solution, demonstrating the versatility and broad range of application of the here proposed model.

Keywords: Electrode effects; Electrolytic plasma; Electrode coverage; Percolation theory; Gas-evolving vertical electrodes.

1. Introduction

Electrode effects have been observed and theoretically analyzed by several authors [1, 2, 3]. Starting from the pioneeristic work of Kellogg [4] it has been observed that at a certain value of voltage between two electrodes in an aqueous electrolyte, there is significant deviation from the standard electrolytic regime: the gas formed at the electrodes, for a critical value of the potential, coalesces, forming a unique continuous gas, which acts as an envelope around the electrodes, giving a sudden drop down in the current at the electrodes, normally followed by a luminous discharge (glow discharge plasma [5, 6]). This process called also electrolytic plasma process has been widely used for practical purpose as surface treatment process for generating oxide coatings on metals, in a similar way to anodizing, but in this case the resulting plasma modifies the structure of the oxide layer [7, 8].

To our knowledge an analytic model describing all this process is still missing. Good reviews on the electrochemical discharges, relevant to its discovery and recent applications, have been published by Gupta et al. [9] and by Wuthrich and Bleuler [10]. In a previous paper Wuthrich and Bleuler proposed also an interesting model for the electrode effects based on the percolation theory [11]. In the same way, our group recently used a percolation approach in order to study the time variation of the photoelectric process during bubbles generation [12]. The goal of the present work is to develop a model for the same effect based on the adsorption phenomenon. The adsorption phenomenon is supposed to be well described by a kinetic equation similar to Langmuir's isotherm, valid in the limit of small adsorption [13]. We assume that the electrical response of the working cell can be described by an electrical circuit formed by a bulk resistance in series with a surface layer characterized by a resistance and a capacitance [14]. Due to the adsorption phenomenon, the surface resistance and capacitance are the parallel of the covered and uncovered parts [15]. In this framework we show that the time dependence of the current contains two characteristics time: one short, related to the charging of the surface layer, and one long related to the kinetics of the coverage. The predictions of the model are validated with experimental data concerning the time dependence of the current and the current-voltage characteristics of a photo-electrolyzer, which is constituted by a $BiVO_4$ photoanode and a Pt cathode assembled in a home-designed cell. In addition, a normalized current-voltage curve is compared with literature data based on another electrolytic applications, in order to assess the

versatility of the developed model.

This paper is organized as follows. In Sect. 2 the electrical response of a simple circuit is considered, to show the divergence of the electric current in an ideal electrochemical cell modeled as a parallel formed by a resistance and a capacitance only. The presence of a bulk resistance on the time dependence of the current is discussed in Sect. 3, whereas the analysis of an electric circuit simulating a real cell is reported in Sect. 4. The influence of the adsorption on the covering effect is considered in Sect. 5, where the kinetic equation used in the analysis is introduced. **In this section a simple expression for the time dependence of the covering ratio, valid when the bulk resistance of the cell is negligible with respect to that of the naked interface layer is deduced.**. The comparison of the theoretical predictions with the experimental data, along with the best obtained fit, is presented in Sect. 6. The final Sect. 7 is devoted to the conclusions.

2. Electrical response of a simple circuit

Let us consider a simple cell whose electrical response to an external excitation can be simulated by an electrical resistance R_s in parallel with a capacitance C_s. When the circuit is submitted to a voltage $V_0(t)$, due to an external power supply, the electric currents in the circuit is $i(t) = i_R(t) + i_C(t)$. In this relation $i_R(t)$ is the conduction current in R_s and $i_C(t)$ the displacement current in C_s (see Fig.1a). By means of simple considerations we get $i_R(t) = V_0(t)/R_s$ and $i_C = C_s dV_0(t)/dt$, and the total current in the circuit is

$$i(t) = \frac{V_0(t)}{R_s} + C_s \frac{dV_0(t)}{dt}. \tag{1}$$

In the particular case in which $V_0(t) = V_0\, u(t)$, where $u(t)$ is the step function such that $u(t < 0) = 0$ and $u(t > 0) = 1$, taking into account that $\delta(t) = du(t)/dt$, where $\delta(t)$ is Dirac's function, from Eq.(1) we obtain

$$i(t) = \frac{V_0}{R_s}\, u(t) + C_s\, V_0\, \delta(t). \tag{2}$$

From Eq.(2) it follows that the $i(t)$ diverges at $t = 0$ and tends to a constant value V_0/R_s, as expected.

3. Real Cell

In a real cell, in the presence of the electrode effect, the electrode is partially covered by bubbles coming from the bulk. In this case, the electrical response of the cell can be simulated by the circuit shown in Fig.1b: the series of a bulk resistance R_b and a surface layer whose resistance, R_s, and capacitance, C_s, are given by

$$R_s = \frac{R_c R_{nc}}{R_c + R_{nc}}, \quad \text{and} \quad C_s = C_c + C_{nc}, \tag{3}$$

where the subscripts c and nc refer to the covered and uncovered part of the electrode. According to (3) the effective resistance and capacitance of the surface layer are the parallel of the surface resistances and capacitances of the covered and uncovered parts [15]. We indicate by λ the thickness of the surface layer, ρ_c and ρ_{nc} the resistivity and by ε_c and ε_{nc} the dielectric constant of the covered and uncovered parts. Indicating by S_c and S_{nc} the surface of the covered and uncovered parts we have

$$R_c = \rho_c \frac{\lambda}{S_c}, \quad \text{and} \quad R_{nc} = \rho_{nc} \frac{\lambda}{S_{nc}}, \tag{4}$$

for the resistances, and

$$C_c = \varepsilon_c \frac{S_c}{\lambda}, \quad \text{and} \quad C_{nc} = \varepsilon_{nc} \frac{S_{nc}}{\lambda}, \tag{5}$$

for the capacitances. If S is the total surface of the electrode, we have the obvious relation $S = S_c + S_{nc}$. If $\beta = S_c/S$ is the coverage of the electrode due to the deposition of the bubbles on it we have $S_c = \beta S$ and $S_{nc} = (1-\beta)S$, and Eq.s(3) can be rewritten as

$$R_s = \frac{R_0}{(1-\beta)[1 + m\beta/(1-\beta)]}, \tag{6}$$

$$C_s = C_0[(1-\beta) + n\beta], \tag{7}$$

where $R_0 = \rho_{nc}(\lambda/S)$ and $C_0 = \varepsilon_{nc}(S/\lambda)$ are the surface resistance and capacitance of the naked electrode.The parameters m and n are defined by $m = \rho_{nc}/\rho_c$ and $n = \varepsilon_c/\varepsilon_{nc}$. Since the presence of the bubbles makes the electrode blocking, $\rho_c \to \infty$, and hence $m \to 0$. Moreover, since $\varepsilon_{nc} \sim 80 \times \varepsilon_0$,

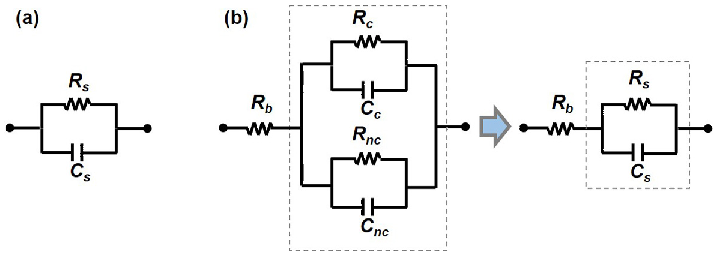

Figure 1: The electrolytic cell is modeled as a parallel formed by a resistance and a capacitance only (a). In order to take into account the coverage effect of the electrode due to the bubbles formation in the electric response of the cell to an electric applied voltage, also the bulk resistance of the cell has to the considered, and the circuit has been modified as reported in the subplot (b)

whereas $\varepsilon_c \sim \varepsilon_0$, $n \sim 1/80$, and can be neglected too. Consequently, from Eq.s (6,7) we get

$$R_s = \frac{R_0}{1-\beta}, \quad \text{and} \quad C_s = (1-\beta)C_0. \tag{8}$$

It follows that the time constant of the surface layer, defined by $\tau_s = R_s C_s = R_0 C_0$, is a constant, independent of the coverage β. We observe that in a working cell β depends on time t, and is regulated by a kinetic equation, as discussed in the following. However, τ_s is time independent.

4. Analysis of the electric circuit simulating a real cell

From the discussion reported above for what concerns the electric response the cell can be simulated by the series of R_b with the parallel (R_s, C_s). When the cell is subjected to an external voltage $V_0(t)$ we have

$$V_0(t) = R_b i(t) + R_s(t) i_R(t), \tag{9}$$

where, as above, $i_R(t)$ is the conduction current across R_s. Furthermore, since R_s and C_s are in parallel we have $R_s i_R(t) = Q/C_s$, where Q is the electrical charge on C_s. From this condition we get $Q = R_s C_s i_R$. The total current in the circuit is then $i(t) = i_R + dQ/dt$, and Eq.(9) can be rewritten, for the discussion reported above about τ_s, as

$$V_0(t) = \left(R_b + \frac{R_0}{1-\beta(t)} \right) i_R(t) + R_b \tau_s \frac{di_R}{dt}. \tag{10}$$

Supposing again that $V_0(t) = V_0 u(t)$, where $u(t)$ is the step function, the solution of Eq.(10), satisfying the initial condition $i_R(0) = 0$ is

$$i_R(t) = \frac{V_0}{R_0 + R_b} \left(1 - e^{-t/\tau}\right), \tag{11}$$

where the effective time constant of the circuit is

$$\tau = \frac{R_b}{R_0 + R_b} \tau_s < \tau_s. \tag{12}$$

We observe that for $t \gg \tau$, but small with respect to the characteristic time related to the covering effect, $i_R \sim V_0/(R_0 + R_b)$.

The total current in the circuit is

$$i(t) = i_R(t) + i_C(t) = \frac{V_0}{R_0 + R_b} \left(1 + \frac{R_0}{R_b} e^{-t/\tau}\right). \tag{13}$$

As expected, $i(0) = V_0/R_b$, whereas $i(0^+) = V_0/(R_0 + R_b)$, where, as before, 0^+ is a time small on the scale of the covering effect, but large with respect to τ. We will write in the following Eq.(13) as

$$i(t) = \frac{V_0}{R_b + R_s(t)} \phi(t), \tag{14}$$

where $\phi(t) = 1 + (R_0/R_b)e^{-t/\tau}$, and $R_s(t) = R_0/[1 - \beta(t)]$. For $t \gg 0^+$ the current in the circuit is given by

$$i(t) = \frac{V_0}{R_b + \{R_0/[1 - \beta(t)]\}}. \tag{15}$$

This means that for $t \gg 0^+$ the time dependence of the current depends only on the kinetics at the electrode, controlling the deposition of the bubbles on it.

5. Kinetic equation for the covering effect

In a working electrotytic cell the coverage is related to the electric charges that during the deposition produce bubbles of gas on the surface. These bubbles change the properties regulating the exchange of charge from the bulk and the external circuit, and hence the electrical properties of the interface

bulk-electrode [15]. We assume that the kinetic of the formation of bubble on the electrode is described by

$$\frac{d\beta}{dt} = A(1-\beta)j - b\beta, \tag{16}$$

where $\beta = S_c/S$ is the coverage. According to Eq.(16) the bubble adsorption can take place only on the uncovered part, and it is proportional to the current density j. As usual, the desorption term is proportional to the surface density of adsorbed bubbles, and hence to the actual coverage β. It is assumed independent of the current density, as proposed in [16, 17]. Kinetic equation (16) is a version of Langmuir's adsorption isotherm [13], discussed in [18]. **It differs from the standard Langmuir's kinetics equation [19, 20]** because the adsorption term is not proportional to the bulk density of adsorbable particles just in front to the electrode, but to the current density at the electrode, that is seems more reasonable in the problem under consideration. The parameters A and b represent the adsorption coefficient and the desorption time, respectively. Rewriting Eq.(14) as

$$j = \frac{i}{S} = \frac{V_0}{r_b + \{r_0/[1-\beta(t)]\}}\,\phi(t), \tag{17}$$

where $r_b = R_b S$ and $r_0 = R_0 S$, Eq.(16) takes the form

$$\frac{d\beta}{dt} = a\,\frac{(1-\beta)^2}{r_0 + r_b(1-\beta)} - b\beta, \tag{18}$$

where $a = AV_0$. The time dependence of β versus t is obtained by integrating Eq.(18). We get

$$\int_0^{\beta(t)} \frac{r_0 + r_b(1-u)}{a(1-u)^2 - bu[r_0 + r_b(1-u)]}du = t, \tag{19}$$

from which $t = t(\beta)$ is obtained. Inverting this equation the time dependence of the coverage is determined. We observe that, as it follows from Eq.(18), $d\beta/dt \to 0$ for $\beta \to \beta_M$ given by

$$\beta_M = \frac{b(r_0 + r_b) + 2a - \sqrt{b[4ar_0 + b(r0 + r_b)^2]}}{2(a + br_b)}. \tag{20}$$

The coverage is a monotonic function of t, such that $\beta(0) = 0$ and $\lim_{t\to\infty}\beta(t) = \beta_M$.

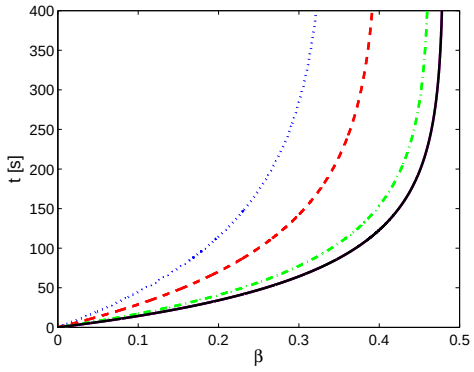

Figure 2: The covering ratio $\beta(t)$ is represented, as defined by Eq.(19), for different values of the ratio r_b/r_0: $r_b = 2r_0$ (blue dotted line), $r_b = r_0$ (red dashed line), $r_b = r_0/5$ (green dash-dot line) and $r_b = 0$ (balk solid line).

In the particular case where $r_0 \gg r_b$ Eq.(18) is well approximated by

$$\frac{d\beta}{dt} = a\,\frac{(1-\beta)^2}{r_0} - b\beta. \tag{21}$$

From Eq.(21) we obtain for the coverage

$$\beta(t) = \frac{\sqrt{4a^2 + b^2 r_0^2} - br_0}{2a}\ \tanh\left\{\frac{\sqrt{4a^2 + b^2 r_0^2} - br_0}{2a}\,t + \operatorname{arctanh}\left(\frac{br_0}{\sqrt{4a^2 + b^2 r_0^2}}\right)\right\}. \tag{22}$$

By means of Eq.(22) the time dependence of the electric current across the cell is easily determined. Of course, the validity of Eq.(22) is limited to the case where the bulk resistance of the cell is negligible with respect to that of the naked interface layer.

In Fig.2 we show the covering ratio $\beta(t)$ given by Eq.(19) for $r_0 = 1.5\,\Omega\times\mathbf{m}^2$, $a = 12 \times 10^{-3}\,\Omega\times\mathbf{m}^2/s$ and $b = 4.5 \times 10^{-3} s^{-1}$, typical of the system considered by us, as discussed in the following, and for $r_b = 2r_0$, $r_b = r_0$, $r_b = r_0/5$ and $r_b = 0$, that corresponds to the case described by Eq.(22). As it is evident from Fig.2, increasing r_b, the effective relaxation time for the covering ratio increases, as expected.

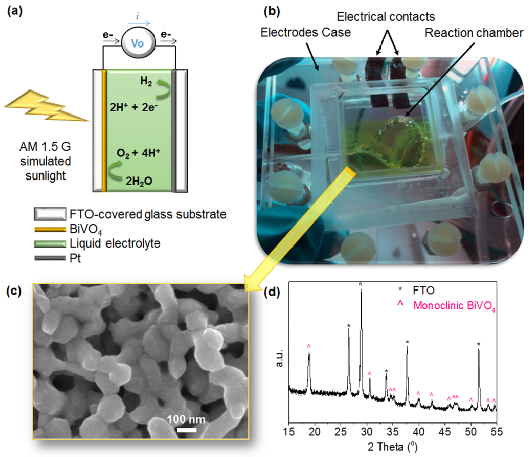

Figure 3: Experimental set-up: Water photo-electrolysis reaction scheme (a). The electrolytic cell (b). FESEM image (c) and XRD analysis (d) showing the $BiVO_4$ morphology and crystal structure.

6. Comparison with experimental results

6.1. Description of the experimental set-up and measurements

The electrical response of an electrochemical cell for the water photo-electrolysis reaction (see Fig.3a) was characterized, in order to use the experimental data for the validation of the here proposed model. In a photo-electrolyzer, water is splitted into its components, i.e. oxygen and hydrogen, mainly using solar energy. A compact home-designed case similar to the one reported in our previous works [21, 22] was used for the experiments, in order to minimize the distance between the electrodes (about 6 mm) thus reducing the ohmic drop in the cell (see Fig.3b).

$BiVO_4$ is a highly studied semiconductor for the sun-driven water splitting due to its ability to exploits the visible part of the solar spectra having a low band gap (of about 2.4 eV), its low-cost and abundance of its components, and its good chemical stability, among others. Thus, a $BiVO_4$ film deposited into a FTO-covered glass (7 Ω/sq, Solaronix) was used for the photo-electrolysis experiments. The so called $BiVO_4/FTO$ was prepared through a metal-organic decomposition (MOD) method [23] with the procedure described elsewhere [12]. In brief, two solutions of $Bi(NO_3)3.5H_2O$ in glacial acetic acid (0.2 M) and $OV(C_5H_7O_2)_2$ in acetylacetone (0.04M) were mixed in a 1 : 1 mole ratio of Bi/V and homogenized on an ultrasound bath

for 30 min. The final solution was spin coated on the FTO-glass substrate ($3 \times 3\,\mathrm{cm}^2$) at 500 rpm for 10 s, then dried in a hot plate at $150°C$ for 5 min and subsequently annealed in an oven at 400°C for 10 min. Six layers were coated following such procedure, followed by a final calcination at 400°C for 2 h in calm air. The $BiVO_4$ morphology (Fig. 3c) was analyzed by means of a MERLIN ZEISS field-emission scanning microscope (FESEM) in top view, evidencing the well sintered $BiVO_4$ nanocrystals of about 85 to 160 nm. The crystalline structure of the photo-anode was analyzed using a PANalytical X'Pert Xray diffractometer in the Bragg-Brentano configuration, using $CuK\alpha$ monochromatic radiation as the X-ray source, with a characteristic wavelength of $\lambda = 1.54059$Å. The XRD analysis (Fig. 3d) confirmed the monoclinic scheelite-like crystalline phase of the $BiVO_4$ electrode (X'Pert HighScore Reference Pattern No. 01-075-1866), which is the most active phase of $BiVO_4$ for the photo-catalytic water oxidation reaction [24, 25]. A Pt thin film was deposited into another FTO-covered glass by sputtering with a Quorum Q150TES instrument at 30 mA for 30 s [12]. The so called Pt/FTO was used as counter, reference and cathodic electrode, while the $BiVO_4/FTO$ was employed as working and anodic photo-electrode.

The experiments were made at ambient temperature using a two-electrodes configuration as shown in Fig. 3a, in a sodium phosphate buffer (0.1 M, pH = 7) electrolyte solution. Amperometric (j, t) curves were recorded applying different voltages (V_0 between 1.8 and 2.5 V) for 5 min, after feeding the reaction chamber with new electrolytic solution, in order to remove all previously formed bubbles from the electrodes surface. The (j, t) curves were recorded under back-side illumination with $AM1.5$ G simulated sunlight spectra at $100\,\mathrm{mW/cm}^2$ of irradiation, by employing a class A solar simulator.

6.2. Fitting of experimental results

In order to set the parameters of Eq.(17) which better approximate the experimental results, it can be useful to study the behavior of the curve $j(t)$ in some particular limits. First of all from the experimental data it can be extracted the value of $j(0)$. From Eq.(17) we have:

$$j(0) = \frac{V_0}{r_b}, \tag{23}$$

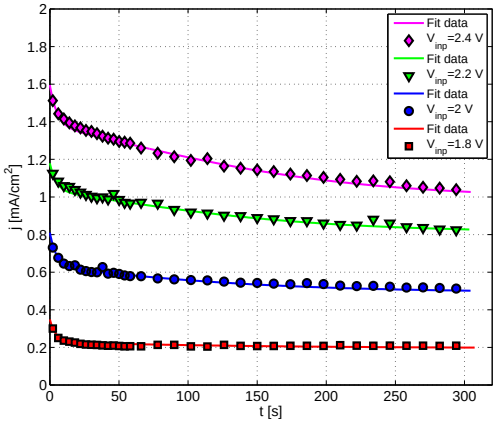

Figure 4: Current density vs. time at different applied potentials (vs. Pt) in the case of the water photo-electrolysis on the $BiVO_4$ electrode under $AM1.5\,\mathrm{G}$ simulated sunlight ($100\,\mathrm{mW/cm^2}$). The lines represent the fitting functions as defined by Eq.(17).

and then the value r_b can be easily estimated. Then, it is possible to approximately define a value $j(0^+)$ as

$$j(0^+) = \frac{V_0}{r_b + r_0}, \tag{24}$$

which can be estimated by taking the intersection in $t = 0$ of the tangent to the experimental curve $j(t)$ in the origin, supposing to disregard the divergence of the current density in the limit $t \to 0$. This point defines the approximate value of r_0.

Supposing $t \gg \tau$ in Eq.(17), so that $\phi(t) \to 0$, and deriving in time, we obtain

$$\frac{dj}{dt} = -V_0 \, \frac{r_0}{[(1-\beta)r_b + r_0]^2} \, \frac{d\beta}{dt}. \tag{25}$$

Using Eq.(16) and considering that $\beta(0) = 0$, we get

$$\left(\frac{d\beta}{dt}\right)_0 = Aj(0), \tag{26}$$

and then combining this equation with Eq.(25) we obtain

$$\left(\frac{dj}{dt}\right)_0 = -\frac{V_0^2}{(r_b + r_0)^3} r_0 A, \tag{27}$$

which defines the value of the adsorption coefficient, A.

Finally, from the asymptotic value of the curve in the limit $t \to \infty$, where $\beta \to \beta_M$, again from Eq.(17) and Eq.(20) we deduce

$$j_M = -\frac{V_0}{\left(r_b + \frac{r_0}{1-\beta_M}\right)}, \tag{28}$$

which sets the remaining free parameter b.

It is then possible to refine the values of these parameters by applying a standard process of best fitting. Note that it is not always possible to invert the result of the integration of Eq.(19) and find an explicit form of $j(t)$. If the case, the fitting process is performed directly on the inverse function $t(j)$.

We have then proceeded to find the fitting parameters in the case of the water photo-electrolysis on the $BiVO_4$ electrode, finding the results shown in Fig.4. Since we have in principle 5 free parameters (r_0, r_b, a, b, τ) for each curve (varying with the external applied voltage), we imposed some additional constrains in order to limit the degrees of freedom of the problem. In particular we imposed a linear dependence on the external applied voltage of the adsorption parameter a and of the desorption time b and a constant value for the characteristic time $\tau = 4.7\,\mathrm{s}$ (this short characteristic time has an influence only in the very first part of the density current curve). Additionally, we have supposed the existence of a threshold in the effect of the applied external potential V_0, as if its effect was diminished by a constant value $V_0' = 0.75V$. We found a posteriori a well defined behavior of the two resistances r_0 and r_b as a function of V_0, as evident from Fig.5. This allows to do some hypothesis on the functions that link these quantities to the applied voltage. We found a very well approximation by stating:

$$r_0 = \frac{\alpha_1}{(V_0 - V_d)^{\beta_1}}, \tag{29}$$

$$r_= \frac{\alpha_2}{(V_0 - V_d)^{\beta_2}}. \tag{30}$$

By knowing the continuous value of the parameters as a function of V_0 it is possible, by combining Eqs.(20) and (28), to give the dependence of the asymptotic value from the applied voltage. Following [11] we normalize this curve in order to obtain the normalized current-voltage characteristic which is a universal curve, independent of the geometry and electrolyte parameters.

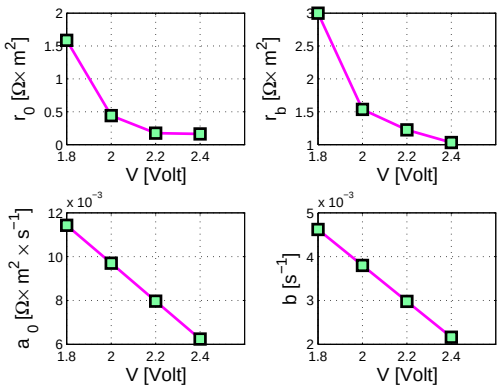

Figure 5: Best fit parameters in the case of the water photo-electrolysis on the $BiVO_4$ electrode, reported in Fig.4.

This is possible by defining the two normalized quantity as follows [11]:

$$\mathcal{J} = \frac{j}{j_{crit}}, \tag{31}$$

$$\mathcal{V} = \frac{V_0 - V_d}{V_{crit} - V_d}, \tag{32}$$

where j_{crit} is the maximum value reached in the current density curve and V_{crit} is the corresponding value of the potential. The value of V_d in our case is set by Eqs.(29) and (30), in [11] represents the sum of the electrode potentials and depends on the electrolyte and electrodes.

The prediction of our model is shown in Fig.6 by the continuous blue line. The red circles are the experimental data presented by Wuthrich and Bleuler in [11], for the electrolysis on stainless steel cylindrical electrodes in NaOH electrolyte; the black squares are taken from Fig.1 in [26], which regard the electrolytic plasma nitrocarburizing of carbon steel discs in an aqueous solution of urea and sodium carbonate. All the data and have been normalized as described in Eqs.(31) and (32). The blue diamonds are the values obtained in our experiments. Our model captures three different regimes: the first linear part (conventional electrolysis), followed by a saturation region and then a third part in which a dramatic decrease of the current density is observed (Kellogg region), in good agreement with different sets of experimental data and observation [11, 26] (also called in literature electrode effects, electrochemical discharges or glow discharge electrolysis [10]). In [11] these three

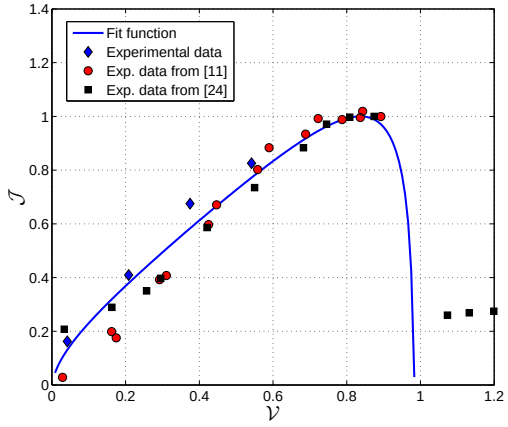

Figure 6: Normalized current–voltage characteristics. Comparison between the experimental results obtained by [11] (red circles), by [26] in their Fig.1 and here normalized (black squares) and by us in the case of the water photo-electrolysis on the $BiVO_4$ electrode (blue diamonds). The continuous blue line represents our model prediction (blue line).

phases are explained by resorting to critical effects in the framework of the percolation theory. In this model the authors describe the electrode as a lattice in which the bubbles formed during electrolysis can adhere to the sites. Two neighboring bubbles on the lattice can form a cluster and eventually detach from the surface. Large bubbles formation increases the resistance between the electrodes. It is known from the percolation theory that when the probability of a lattice site to be occupied reaches a critical value (then the electrode is shield by a critical layer of bubbles) then there is the transition to a new phase in which the clusters coalescence in a unique infinite cluster. This phase corresponds to the formation of a gas film covering almost the whole electrode surface, causing a dramatic decrease of the current density in the circuit. In a recent paper [12], using a percolation model, the progress to the infinite cluster is described by two different type regimes seen as a slope change of the tangent to the current versus time graphic at the moment corresponding to the percolation threshold. Whereas in the adsorption model the unique infinite cluster is achieved in a smooth manner, in the percolation model there could be more clusters that overpass the threshold, leading to a description of several large bubbles that can eventually detach from the electrode.

7. Conclusions

We have proposed a model for the electrode effects based on the adsorption mechanism. It has been assumed that the electric response of a working electrochemical cell is well described by a simple circuit formed by a bulk resistance in series with a surface layer characterized by a resistance in parallel with a condenser due to the properties of the liquid-electrode interphase. During the formation of the bubbles on the electrode, the electrical properties of the interface change. In particular, the formation of bubbles has been modeled by a kinetic equation at the interface, where the adsorption term, supposed proportional to the current density, describes the formation of the bubbles on the electrode, whereas the desorbing term takes into account the detachment of the bubbles from it. By means of the kinetic equation at the electrode, the time dependence of the electric current across photo-electrolytic cell based on a $BiVO_4$ photoanode was evaluated, as well as its dependence on the applied voltage. The comparison of the current-voltage characteristic predicted by our model is in good agreement with the experimental results here reported for the photo-electrolysis, and reported in the literature for both electrolysis [11] and electrolytic plasma nitrocarburizing of carbon steel electrodes [26], which demonstrate the broad range of applications for which the here presented model could be used.

Acknowledgment. Many thanks are due to N. Penazzi for useful discussion and to Mauro Raimondo for performing FESEM measurements. The financial support from the European Commission on the 7th Framework Program (NMP-2012 Project Eco2CO2 nr.309701 and FCH-JU Call 2011-1 Project ArtipHyction nr.303435) is gratefully acknowledged.

[1] H. Vogt, Contribution to the interpretation of the anode effect. Electrochimica Acta, **42** (1997) 2695-2705.

[2] H. Vogt, The anode effect as a fluid dynamic problem. J. Appl. Electrochem. **29** (1999) 137-14

[3] H. Vogt, J. Thonstad, The voltage of alumina reduction cells prior to anode effect. J. Appl. Electrochem. **32** (2002) 241-249

[4] H. H. Kellogg, Anode Effect in Aqueous Electrolysis. J. Electrochem. Soc. **97** (1950) 133-142.

[5] A. Hickling, Modern Aspects of Electrochemistry, vol. 6, Butterworths, London, 1971, p. 329.

[6] A. Hickling, M.D. Ingram, Contact glow-discharge electrolysis. Trans. Faraday Soc. **60** (1964) 783.

[7] Y.N. Tyurin, A.D. Pogrebnyak, Specific features of electrolytic-plasma quenching. Tech. Phys. **47** (2002) 1463.

[8] A.L. Yerokhin, X. Nie, A. Leyland, A. Matthews, S.J. Dowey, Plasma electrolysis for surface engineering. Surf. Coat. Technol. **122** (1999) 73 .

[9] P. Gupta, G. Tenhundfeld, E. O. Daigle, and D. Ryabkov, Surf. Coat. Technol. **201**, 8746 (2007)

[10] R. Wüthrich and P. Mandin, Electrochemical discharges - Discovery and early applications. Electrochimica Acta **54** (2009) 4031-4035.

[11] R. Wüthrich and H. Bleuler, A model for electrode effects using percolation theory. Electrochimica Acta **49** (2004) 203-207.

[12] S. Hernández, G. Barbero, G. Saracco, A.L. Alexe-Ionescu, Considerations on Oxygen Bubbles Formation and Evolution on BiVO4 Porous Anodes Used in Water Splitting Photoelectrochemical Cells. The Journal of Physical Chemistry C (2015) DOI: 10.1021/acs.jpcc.5b01635 .

[13] John O'M. Bockris, Amulya K. N. Reddy, and Maria Gamboa-Aldeco, "*Modern electrochemistry*", volume 2, Kluwer Academic/Plenum Publishers, New York (2003).

[14] G. Barbero, P. Batalioto, and Figueiredo A. M. Neto, Impedance spectroscopy of an electrolytic cell limited by ohmic electrodes. J. Appl. Phys. **101** (2007) 054102.

[15] G. Saracco, A. L. Alexe-Ionescu, and G. Barbero, Differential conductance of an electrolytic cell in the presence of deposition of a coating material on the electrode. J. of Electroanal. Chem. **741** (2015) 134-139.

[16] J. Venczel, Über den gasblasen bei elektrochemischen prozessen. Electrochimica Acta **15** (1970) 1909-1920 .

[17] H. Vogt, The problem of the departure diameter of bubbles at gas-evolving electrodes. Electrochim. Acta **34** (1989) 1429-1432

[18] G. Barbero, Influence of adsorption phenomenon on the impedance spectroscopy of a cell of liquid. Phys. Rev. E **71** (2005) 062201.

[19] A. Islam, M. R. Khan, and S. I. Mozumder, Chem. Eng. and Technology, **27**, 1095 (2004).

[20] Yu Liu and Liang Shen, Langmuir **24**, 11625 (2008).

[21] S. Hernández, G. Saracco, A.L. Alexe-Ionescu, G. Barbero, Electric investigation of a photo-electrochemical water splitting device based on a proton exchange membrane within drilled FTO-covered quartz electrodes: under dark and light conditions. Electrochimica Acta (2014) **144** 352-360.

[22] S. Hernández, M. Tortello, A. Sacco, M. Quaglio, T. Meyer, S. Bianco, G. Saracco, C.F. Pirri, E. Tresso, New Transparent Laser-Drilled Fluorine-doped Tin Oxide covered Quartz Electrodes for Photo-Electrochemical Water Splitting. Electrochimica Acta, **131** (2014) 184-194.

[23] W. Luo, Z. Li, T. Yu, Z. Zou, Effects of surface electrochemical pretreatment on the photoelectrochemical performance of Mo-doped $BiVO_4$. The Journal of Physical Chemistry C, **116** 5076-5081 (2012).

[24] Y. Park, K.J. McDonald, K.-S. Choi, Progress in Bismuth Vanadate Photoanodes for Use in Solar Water Oxidation. Chemical Society Reviews **42** (2013) 2321-2337.

[25] C. Martinez Suarez, S. Hernández, N. Russo, Applied Catalysis A: General, (2015) DOI: 10.1016/j.apcata.2014.1011.1044.

[26] M.K. Zarchi, M.H. Shariata, S.A. Dehghana, and S. Solhjoo, Characterization of nitrocarburized surface layer on AISI 1020 steel by electrolytic plasma processing in an urea electrolyte. J. Mater. Res. Technol. **2**(3) (2013) 213-220.